

A national ground motion amplification model for Switzerland based on site proxies and incorporating local response observations at instrumented sites

Conference Paper

Author(s):

[Bergamo, Paolo](#) ; [Panzera, Francesco](#) ; [Cauzzi, Carlo Virgilio](#) ; [Glueer, Franziska](#) ; [Perron, Vincent](#) ; Fähr, Donat

Publication date:

2022-09

Permanent link:

<https://doi.org/10.3929/ethz-b-000594281>

Rights / license:

[In Copyright - Non-Commercial Use Permitted](#)



A national ground motion amplification model for Switzerland based on site proxies and incorporating local response observations at instrumented sites

Paolo Bergamo – Swiss Seismological Service (SED) at ETH Zurich, Zurich, Switzerland,
paolo.bergamo@sed.ethz.ch

Francesco Panzera – Swiss Seismological Service (SED) at ETH Zurich, Zurich, Switzerland,
francesco.panzera@sed.ethz.ch

Carlo Cauzzi – Swiss Seismological Service (SED) at ETH Zurich, Zurich, Switzerland,
carlo.cauzzi@sed.ethz.ch

Franziska Glüer – Swiss Seismological Service (SED) at ETH Zurich, Zurich, Switzerland,
franziska.glueer@sed.ethz.ch

Vincent Perron – Swiss Seismological Service (SED) at ETH Zurich, Zurich, Switzerland,
vincent.perron@sed.ethz.ch

Donat Fäh – Swiss Seismological Service (SED) at ETH Zurich, Zurich, Switzerland,
donat.fah@sed.ethz.ch

Abstract: Mapping the site response of strong ground motion is one of the key steps for earthquake risk assessment studies. In the wider framework of the national ‘Earthquake Risk Model for Switzerland’ project, we have prepared a ground motion site amplification model covering entire Switzerland. The model includes amplification maps for peak ground velocity (PGV), pseudo-spectral acceleration (PSA) at $T = 1.0, 0.6, 0.3$ s and corresponding uncertainties. The amplification maps for PGV, PSA(1.0s) and PSA(0.3s) have been also translated into macroseismic intensity aggravation layers for their use in ShakeMaps representations. The site response model we have developed is based on the local earthquake amplifications measured by 280 seismic stations deployed across Switzerland and retrieved by means of the empirical spectral modelling technique. The local estimates of site response are then spread over the national territory resorting to a geological classification, multi-scale topographical slope and the inferred depth-to-bedrock as predictor layers for the extrapolation. The local measures of site amplification are embodied in the national model using a regression-kriging algorithm. Considering that a significant portion of the seismic stations is located in urban environment, this inclusion contributes to the accuracy of the estimation of site response in areas with high exposure and it locally reduces its associated uncertainty.

Keywords: risk assessment, site amplification, national model, site-condition indicators, regression

1. Introduction

Mapping the site response of strong ground motion is one of the key steps for earthquake risk assessment studies. Local, accurate site amplification models are generally obtained in the framework of microzonation studies (e.g. Lchet et al., 1996, Michel et al. 2017, Hailemikael et al., 2020; Panzera et al., 2022). On the other hand, for a large-scale (e.g. national scale) site response layer the approach is generally more approximate, and can consist in mapping proxies for site amplification (e.g. average V_s in the surficial 30 m, V_{s30}), using topographical and/or geological indicators (Yong et al., 2012, Vilanova et al.

2018, Li et al., 2022). More recently, however, works such as Weatherill et al. (2020), have introduced the possibility to directly map the local amplification at large spatial scale from indirect site condition parameters. Following this example, in this study we describe the strategy we have implemented to produce a set of maps representing the earthquake site amplification for various ground-motion measures (PGV, PSA(1.0s), PSA(0.6s), PSA(0.3s)) and their associated uncertainties. The maps cover the entire Switzerland with a resolution of 25 m, and they are part of the “Earthquake Risk Model Switzerland” project, http://www.seismo.ethz.ch/en/research-and-teaching/ongoing-projects/#pr_00056.xml. The maps have been obtained by extrapolating the local site amplification measurements provided by seismic stations, resorting to site condition indicators (lithology, topographical slope, estimated bedrock depth) as predictor variables. Local site response measurements provided by instrumented sites are incorporated into the amplification model by means of regression kriging (RK, Hengl et al., 2007), increasing the local accuracy of the maps and decreasing their uncertainty.

2. Dataset of site response measurements from instrumented sites

The local earthquake response was estimated at Swiss instrumented sites by means of the empirical spectral modelling technique (Edwards et al., 2013). The method is based on comparison, at each event, between the Fourier spectrum measured at the considered seismic station and the corresponding spectrum modelled according to the ground-motion Swiss stochastic model of Edwards and Fäh (2013). The latter models source and path terms, and then propagates the ground motion up to a standard rock outcrop having V_{s30} of 1100 m/s (Swiss standard rock model, Poggi et al., 2011). The observed ratio between measured and modelled spectra is then interpreted as representing the local earthquake response of the site hosting the station, relative to that of the reference standard rock outcrop.

This comparison between empirical and modelled spectra is routinely carried out after each event at the Swiss Seismological Service (SED) since 2018, and it has been retroactively applied to all events from 2001 onwards. This operation allows retrieving the Fourier site amplification function at virtually all the instrumented sites of the Swiss networks. As the stations record an increasing number of events over time, the amplification function representative of each site is obtained as the geometrical average of the single-event amplification functions (Fig. 1, top left panel). Processing all regional earthquakes from the period 2001 – 2021, we have been able to attribute an inelastic Fourier site amplification function, constrained by at least 5 events in the range 0.5 – 10 Hz, to 280 (urban) free-field stations (Fig. 1, bottom panels).

Finally, for compatibility with the other modules of the ‘Earthquake Risk Model for Switzerland’ (hazard and fragility modules), the Fourier amplifications are translated to PSA amplifications resorting to random vibration theory (RVT, Boore, 2003; see Fig. 1, top right panel). Similarly to Poggi and Fäh (2015), the conversion to PSA (and PGV) amplification is performed computing the ratio between the pseudo-response spectra obtained first including and then removing the Fourier local amplification of the target site. The earthquake scenarios employed for the RVT simulations are drawn from the most recent hazard model for Switzerland (Wiemer et al., 2016). For the purpose of our work, we finally stored the retrieved amplification values for PGV, PSA(1.0s), PSA(0.6s) and PSA(0.3s) and associated uncertainties in a unified database.

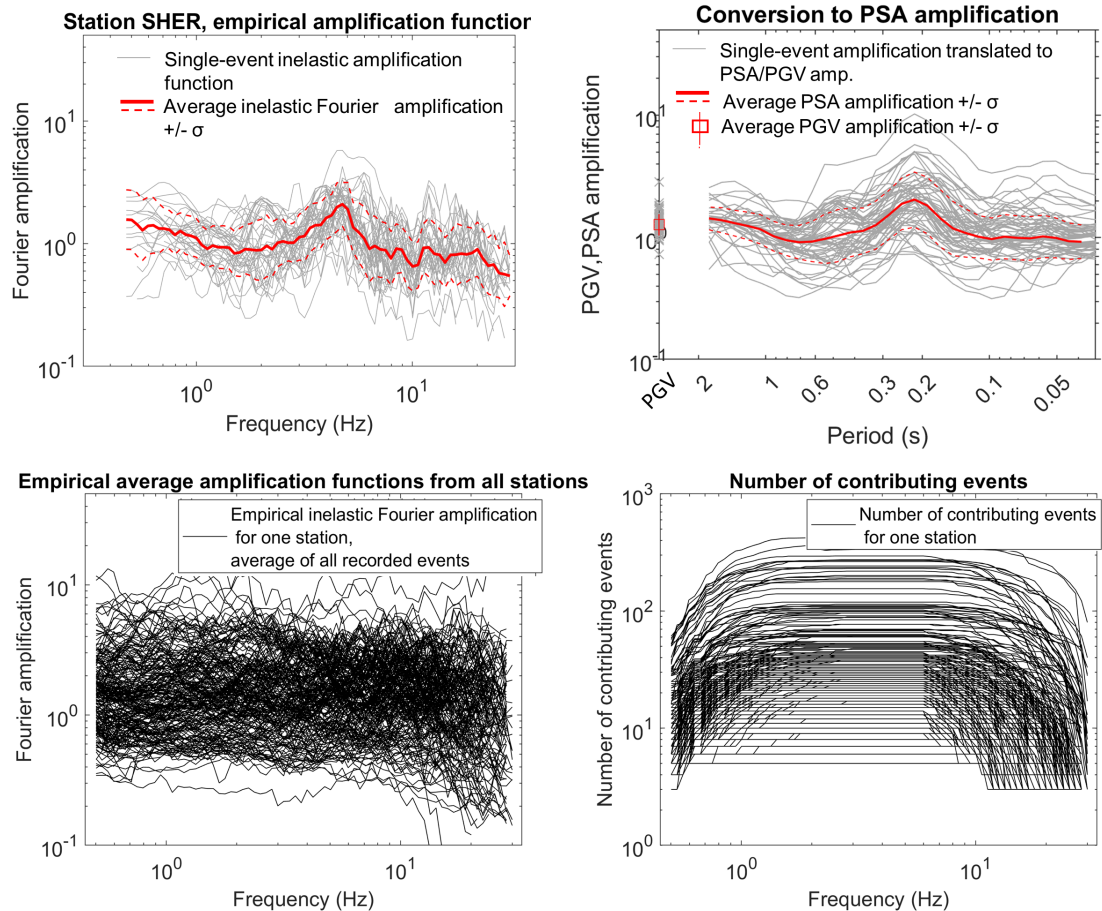


Fig. 1 – Top left: empirical Fourier amplification function obtained using the empirical spectral modelling technique for the strong motion station SHER, installed in Hérémece, south-west Switzerland. Top right panel: conversion of the Fourier amplification into PGV, PSA amplification with random vibration theory. Bottom, left panel: average Fourier empirical amplification functions extracted at 280 (urban) free-field stations in Switzerland and constrained by at least 5 events in the range 0.5 – 10 Hz. Bottom right panel: number of events contributing to the average amplification function at each station.

3. Layers of site condition indicators

For the extrapolation of the high-quality (but local) information provided by the empirical amplification functions from instrumented sites, we resorted to site condition proxies (SCPs) as predictor variables. Several studies in literature have evidenced the correlation between topographical and geological indicators (which can be retrieved from layers of diffuse information such as digital elevation models and geological maps) and geophysical parameters related to site response (e.g. Vs30, Wald and Allen, 2007). More recent works have proven that topographical and geological indicators can also be directly linked to site amplification (Weatherill et al., 2020). Based on existing literature and our own studies on Switzerland (Bergamo et al., 2021), we selected the following site condition indicators:

- A lithologic classification of Switzerland, based on the 1:500000 national geological map (Swisstopo, 2005) and on the works of Zappone and Kissling (2021) and Panzera et al. (2021; see Fig. 2, upper panel).

- Multi-scale maps of the topographical slope (e.g. Fig. 2, lower left panel), derived from the digital height model DHM25 (Swisstopo, 1999) covering Switzerland with a regular grid of 25 x 25 m cells. We computed the topographical slope at the following spatial scales: 75, 125, 275, 600, 1000, 1800, 3600 m.

- The estimated depth to bedrock, obtained from the bedrock elevation model by the Swiss Federal Office of Topography (Swisstopo, 2019), covering Switzerland almost entirely (Fig. 2, lower right). The reliability of this dataset for site response prediction was assessed by comparing its estimated depth values with depths of the engineering bedrock (H800) as measured by ~225 Vs profiles from site characterization surveys (Michel et al., 2014, Hobiger et al., 2021). The comparison highlighted a good agreement for predicted values of bedrock depth (from Swisstopo model) larger than a few meters; areas with predicted depths < 3 m were discarded from the map (grey area in Fig. 2, lower right).

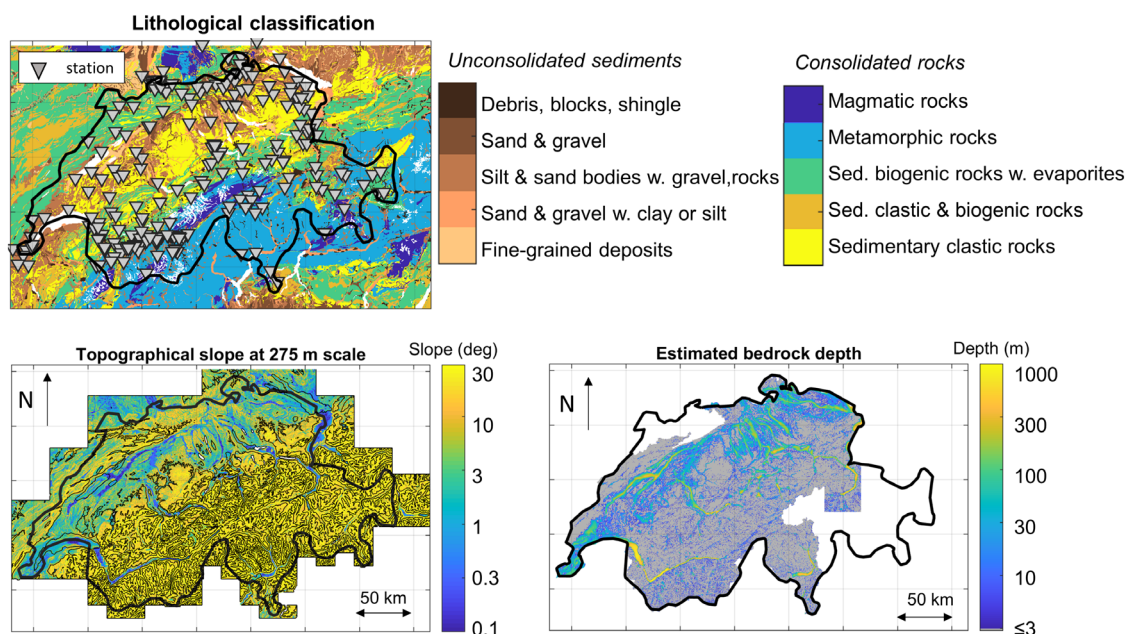


Fig. 2 – Employed site condition indicators. Top left: map of the adopted simplified lithologic classification and location of the 280 (urban) free-field station with empirical amplification function. Bottom left: topographical slope at the spatial scale of 275 m. Bottom right: map of bedrock depth derived from the Swisstopo 2019 model; predictions < 3 m are not considered reliable and are highlighted in grey. Blank areas are not covered by the Swisstopo model.

We retrieved the values of the SCPs listed above at the sites of the 280 (urban) free-field stations with estimated local amplification values. A sensitivity analysis correlating PGV, PSA(1.0s), PSA(0.6s) and PSA(0.3s) amplifications with the topographical slopes at various scales identified the slope at the extent of 275 m as the one achieving the highest correspondence with the considered amplifications.

4. Workflow for the mapping of site response

Once compiled the joint datasets of measured site amplifications and of the layers of local condition parameters (Chapters 2, 3), these were combined for the mapping the PGV,

PSA(1.0s), PSA(0.6s) and PSA(0.3s) amplification across all Switzerland. The approach we followed for each intensity measure type involves three successive steps:

- First, amplification-*vs*-slope (at 275 m scale) and amplification-*vs*-bedrock depth relationships are retrieved for each lithotype hosting ≥ 10 stations (see Chapter 3). As far as amplification-*vs*-slope regressions are concerned, this condition is satisfied for all but one lithotype ('magmatic rocks', marginal from the risk point of view, for which no amplification predictions are eventually provided). Regarding the amplification-*vs*-bedrock depth relations, as the bedrock model does not cover all Switzerland, such regressions are available for only a subset of lithotypes (see examples in Fig. 3, top row). Only for the lithotype "sand and gravel with clay or silt" (alluvial sediments), hosting the highest number of stations (60), a bivariate smoothing-spline surface correlating amplification with slope and bedrock depth can be reliably constrained (Fig. 3, middle row). For each of such lithotype-specific relationships, the coefficient of determination r^2 and the standard deviation of the spatially uncorrelated residuals are computed.

- An amplification prediction is attributed to each 25 x 25 m cell of a raster map covering the entire Switzerland, entering the amplification-*vs*-slope and amplification-*vs*-bedrock depth (if available) regressions with the values of slope and bedrock depth at the considered cell. If two valid predictions are available (from topographic slope and bedrock depth), the one issued from the regression with higher r^2 is preferred. A joint map representing the uncertainty of the prediction is also created, filled with the values of standard deviations of uncorrelated residuals of the relationships used for the prediction.

- The spatial correlation of the residuals of the amplification-*vs*-proxy relationships is evaluated by computing their semivariograms (Fig. 3, bottom row). These evidenced a spatial correlation within ranges of about 8 km for PGV and PSA(1.0s), decreasing to ~ 6 km for PSA(0.6s) and ~ 2 km for PSA(0.3s). We exploited this spatial correlation to implement a final correction of the amplification prediction for the map cells having distance $<$ range from the closest station(s). This correction is performed following the regression kriging (RK) algorithm, and can be described as a weighted mean of the residual(s) at the neighbouring station(s); at the same time, the local uncertainty is also decreased by a weighted mean of the expected covariances between the map cell and the surrounding station(s). This final RK correction allows to locally constrain the amplification prediction to the measured values in the surrounding area and to locally reduce the prediction uncertainty.

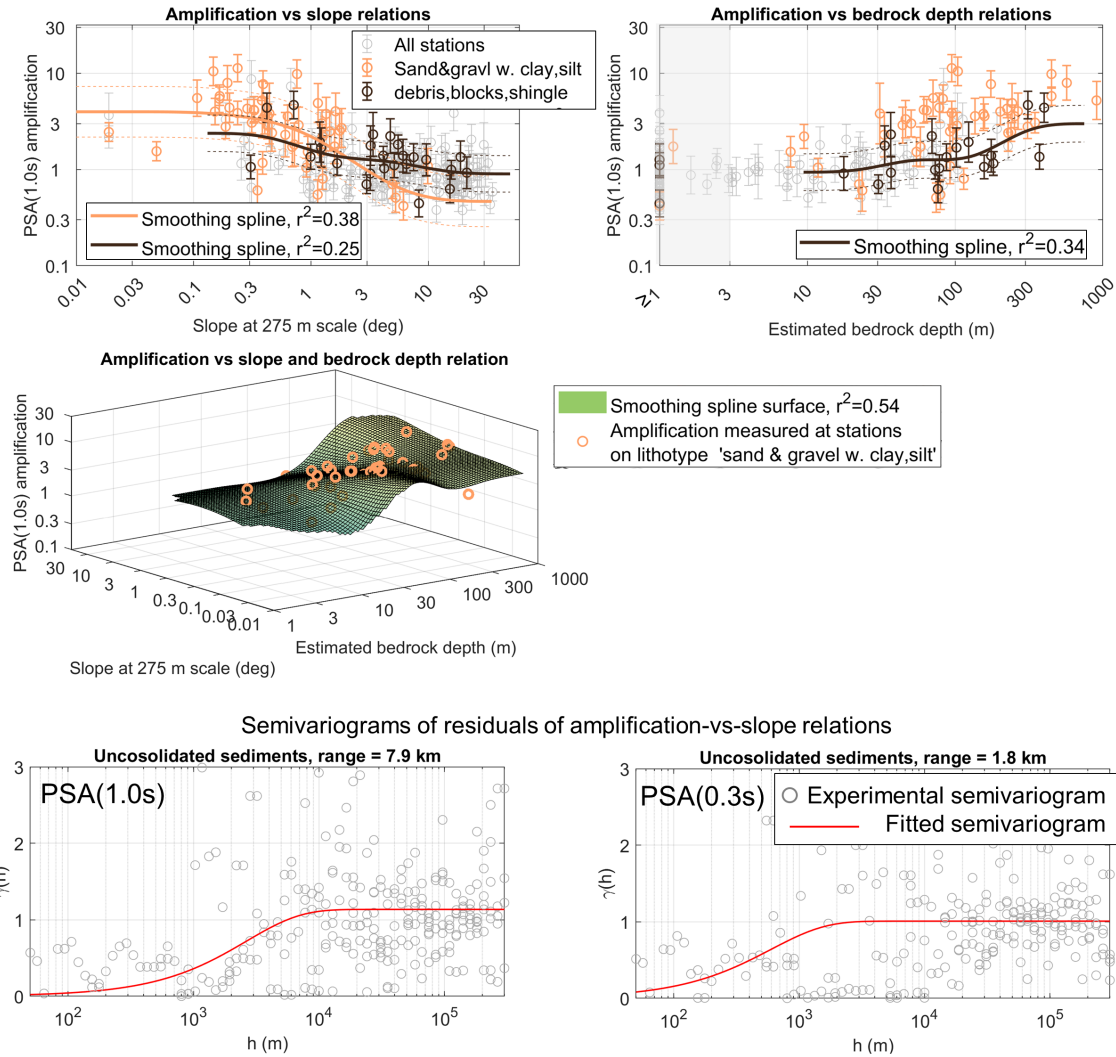


Fig. 3 – Top row: examples of amplification-*vs*-slope (left) and amplification-*vs*-bedrock depth (right) relationships for sample lithotypes. Center row: bivariate regression of amplification-*vs*-slope and -bedrock depth, evaluated only for the ‘sand and gravel with clay or silt’ lithotype, hosting the highest number of stations. Bottom row: semivariograms of the residuals of amplification-*vs*-slope relations for unconsolidated lithotypes for PSA(1.0s) (left) and PSA(0.3s) (right).

5. Obtained amplification model and assessment of its uncertainties

The results we obtain from the workflow illustrated in Chapter 4 is a set of maps representing the site amplification term for PGV, PSA(1s), PSA(0.6s) and PSA(0.3s) and a joint set of maps of the corresponding prediction uncertainties (see examples in Fig. 4, top row).

For the integration of the produced site response layer in the wider framework of the Earthquake Swiss Risk model, we carried out a complete assessment of its uncertainties, and we related them to the variability terms of the Swiss stochastic ground-motion model of Edwards and Fäh (2013). This operation allows incorporating the uncertainties of the site response module in the adopted stochastic model for the prediction of ground motion, hence avoiding double-counting of uncertainties in the final risk model. In the model of Edwards and Fäh (2013), the total uncertainty of the GMPE (σ) is composed of three items:

$$\sigma = (\tau^2 + \varphi_{S2S}^2 + \varphi_{SS}^2)^{0.5} \quad (1)$$

where τ is the between-event variability, φ_{S2S} is the site-to-site variability and φ_{SS} is the single-site within-event variability. We addressed the two terms related to local response, i.e. φ_{S2S} and φ_{SS} . As illustrated in Chapter 4, the national amplification layers are obtained defining observed amplification-*vs*-slope and/or -inferred bedrock depth relations for each lithotype; these relations are then mapped over the entire surface of Switzerland. Consistently with this approach, we identified the variability around the fitted smoothing spline of spatially uncorrelated stations (i.e. the prediction uncertainty mapped in Fig. 4, upper right panel) as the model's site-to-site variability (φ_{S2S}). In other words, the variability observed within each lithotype, given the topographic slope and/or the inferred bedrock depth as predictor variable(s), can be assumed as expressing the model's φ_{S2S} .

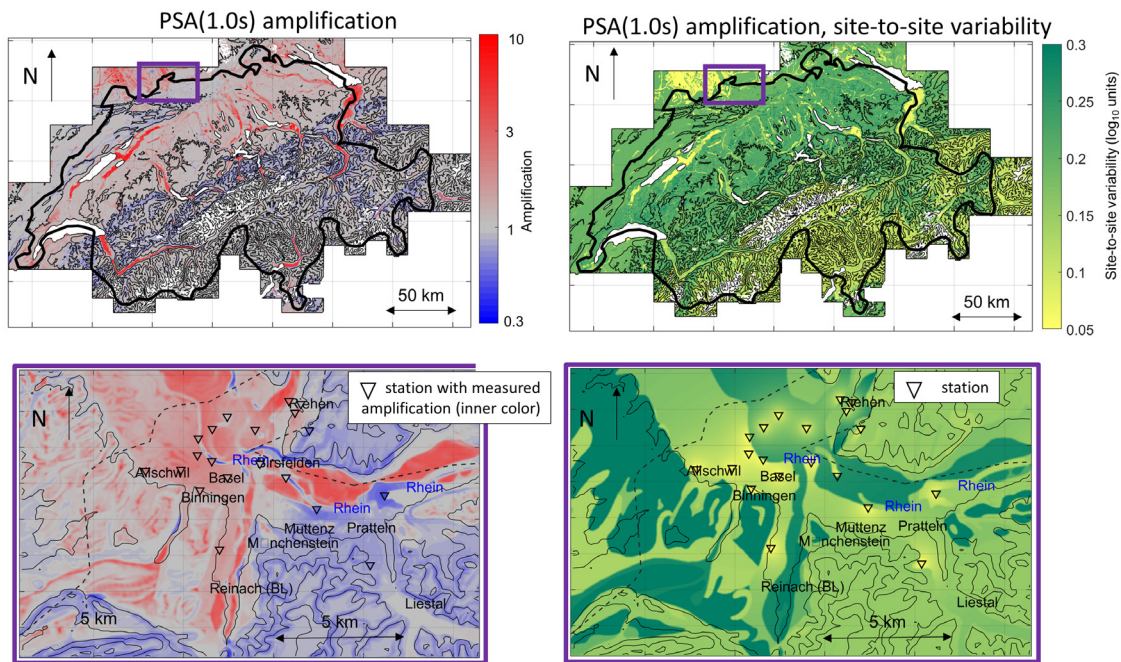


Fig. 4 – Example of obtained results. Top: obtained amplification map for PSA(1.0s) (left) and map of related uncertainty (right), identified as the site-to-site variability of the stochastic model of Edwards and Fäh (2013). Bottom row: zoom on the area of the city of Basel. The amplification prediction collapses to the observed amplification at and around the seismic stations (left), while the uncertainty collapses to 0 (right).

For the representation of the single-site within-event variability (φ_{SS}), we associated the latter with the variability observed across the single-event amplification functions estimated for the Swiss stations with empirical spectral modelling technique and RVT (e.g. Fig. 1, upper right panel). We observed that the standard deviation over the single-event amplifications at the same site does show a mild correlation with the lithotype, i.e. softer geomaterials have wider variability and vice versa stiffer lithologies have narrower uncertainties; therefore, to map φ_{SS} we attributed to each lithotype the average standard deviation of the empirical amplification functions of the stations falling on that lithotype. It should be noted that in comparison to φ_{S2S} , the values of φ_{SS} determined for the various lithologic units show a narrower variability (they are generally comprised between 0.1 - 0.2 log₁₀ units for PSA(1.0s), see Fig. 5 and compare with Fig. 4, upper right panel). φ_{SS} also globally increases as the period decreases.

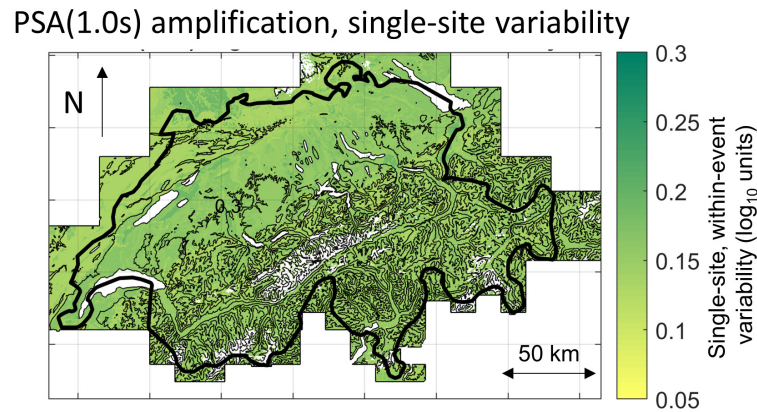


Fig. 5 – Estimated map of single-site, within-event variability for PSA(1.0s) amplification.

6. Conclusions

We describe the strategy we have implemented to produce a set of maps representing the earthquake site amplification for various ground-motion parameters (PGV, PSA(1.0s), PSA(0.6s), PSA(0.3s)) and their associated uncertainties. The maps cover the entire Switzerland with a resolution of 25 m, and they are part of the “Earthquake Risk Model Switzerland” project. The maps have been obtained by extrapolating the local site amplification measurements provided by seismic stations, resorting to site condition indicators (lithology, topographical slope, estimated bedrock depth) as predictor variables. Local site response measurements provided by instrumented sites are incorporated into the amplification model by means of regression kriging, increasing the local accuracy of the maps and decreasing their uncertainty. Future steps in our work are related to the validation of these maps: i) by comparing their prediction with local response measurements by seismic stations not included in the calibration dataset; ii) by collating the national site response layer with local amplification models obtained from dedicated studies (e.g. Perron et al., 2020, Panzera et al. 2022, Janusz et al., 2021); iii) after converting the PGV, PSA(1.0s) and PSA(0.3s) amplification maps to macroseismic aggravation with relations from literature (Faenza and Michelini 2010, 2011, Michel et al. 2017), by comparing the predicted macroseismic intensity with intensity measures from past earthquakes.

Acknowledgements

The authors acknowledge financial support within the framework of the project ERM-CH Swiss Earthquake Risk Model (financed by the Swiss Federal Office for the Environment, the Federal Office for Civil Protection and ETH Zurich).

References

- Bergamo et al. (2021). Correspondence between site amplification and topographical, geological parameters: collation of data from Swiss and Japanese stations and neural networks-based prediction of local response. BSSA, doi: 10.1785/0120210225
- Boore, D. (2003). Simulation of ground motion using the stochastic method. *Pure and applied Geophysics*, 160:635–676, 2003.
- Edwards, B. et al. (2013). Determination of site amplification from regional seismicity: Application to the Swiss National Seismic Networks, *Seismol. Res. Lett.* 84(4) 611–621.

- Edwards B. and Fäh, D. (2013). A stochastic ground-motion model for Switzerland. *Bulletin of the Seismological Society of America*, Vol. 103, No. 1, pp. 78–98
- Faenza L., Michelini A. (2010). Regression analysis of MCS intensity and ground motion parameters in Italy and its application in ShakeMap. *Geophys. J. Int.* 180(3), 1138–1152.
- Faenza L., Michelini A. (2011). Regression analysis of MCS intensity and ground motion spectral accelerations (SAs) in Italy. *Geophys. J. Int.* 186(3), 1415–1430.
- Hailemikael, S., Amoroso, S. & Gaudiosi, I. (2020). Guest editorial: seismic microzonation of Central Italy following the 2016–2017 seismic sequence. *Bull Earthquake Eng* 18, 5415–5422 (2020).
- Hengl T. et al. (2007). About regression-kriging: From equations to case studies, *Computers & Geosciences*, Volume 33, Issue 10, Pages 1301–1315.
- Hobiger et al. (2021). Site Characterization of Swiss Strong-Motion Stations: The Benefit of Advanced Processing Algorithms, *BSSA* 111 (4): 1713–1739.
- Janusz. P. et al., (2021). Evaluation of seismic site response in urban areas: insight from the case of Lucerne, Switzerland. The 6th IASPEI / IAEE International Symposium: Effects of Surface Geology on Seismic Motion August 2021, extended abstract G95-P095.
- Michel C. et al. (2014). Assessment of Site Effects in Alpine Regions through Systematic Site Characterization of Seismic Stations, *BSSA* 104 (6): 2809–2826.
- Michel C. et al. (2017). Site amplification at the city scale in Basel (Switzerland) from geophysical site characterization and spectral modelling of recorded earthquakes. *Physics and Chemistry of the Earth Parts A/B/C* 98:27–40.
- Lachet, C. et al. (2016). Site effects and microzonation in the city of Thessaloniki (Greece) comparison of different approaches. *Bulletin of the Seismological Society of America*; 86 (6): 1692–1703
- Li M. et al. (2022). Texas-specific VS30 map incorporating geology and VS30 observations. *Earthquake Spectra*. 2022;38(1):521-542
- Panzera et al. (2021). Canonical Correlation Analysis Based on Site-Response Proxies to Predict Site-Specific Amplification Functions in Switzerland. *BSSA* (2021) 111 (4): 1905–1920.
- Panzera, F, Alber, J, Imperatori, W, Bergamo, P, Fäh, D (2022). Reconstructing a 3D model from geophysical data for local amplification modeling: The study case of the upper Rhone valley, Switzerland, *Soil Dynamics and Earthquake Engineering*, 155, 107163, <https://doi.org/10.1016/j.soildyn.2022.107163>
- Perron, V. et al., (2020). "Empirical earthquake's site response assessment in the Sion area, Switzerland", in: 18th Swiss Geoscience Meeting Zurich 2020, Zürich, Switzerland
- Poggi V. and Fäh, D. (2015). A proposal for horizontal and vertical elastic design spectra Input for the new Swiss code for dams. Technical Report SED/BFE/R/01/30072015
- Poggi, et al. (2011). Derivation of a reference shear-wave velocity model from empirical site amplification, *Bull. Seismol. Soc. Am.* 101(1) 258–274.
- Swisstopo, Swiss Federal Office of Topography (1999). Digital Height Model DHM25, <https://www.swisstopo.admin.ch/it/geodata/height/dhm25.html>
- Swisstopo, Swiss Federal Office of Topography (2005). Geological Map of Switzerland 1:500000 (GK500) https://data.geo.admin.ch/ch.swisstopo.geologie-geologische_karte
- Swisstopo, Swiss Federal Office of Topography (2019). Grossezza da la crappa lucca da la Svizra, <https://www.swisstopo.admin.ch/it/geodata/geology/models/unconsolidated-deposits.html>
- Vilanova S. P. et al. (2018). Developing a Geologically Based Vs30 Site-Condition Model for Portugal: Methodology and Assessment of the Performance of Proxies, *Bull. Seismol. Soc. Am.*, 108(1) 322–337
- Wald, D. J., and T. I. Allen (2007). Topographic slope as a proxy for seismic site conditions and amplification, *Bull. Seismol. Soc. Am.* 97(5) 1379–1395.
- Weatherill, G., et al. (2020). Re-thinking site amplification in regional seismic risk assessment, *Earthquake Spectra* 36(S1) 274–297.
- Wiemer S. et al. (2016). Seismic Hazard Model 2015 for Switzerland (SUIhaz2015), Swiss Seismological Service (SED) at ETH Zurich.
- Yong A. et al. (2012). A Terrain-Based Site-Conditions Map of California with Implications for the Contiguous United States. *BSSA* 102(1):114–128.
- Zappone A. and E. Kissling (2021). SAPHYR: Swiss Atlas of Physical Properties of Rocks: the continental crust in a database, *Swiss J Geosci* (2021) 114:13